

## Muscle disease in severe COVID-19 patients: a microangiopathic myopathy

Josep Lloreta-Trull , Judith Marin-Corral , Nuria Juanpere , Sergi Pascual-Guardia , Javier Gimeno , Dolores Naranjo , Laura Segalés , Silvia Hernández , Mercedes Simón , Laia Serrano , Beatriz Casado , Belén Lloveras & Joaquim Gea

**To cite this article:** Josep Lloreta-Trull , Judith Marin-Corral , Nuria Juanpere , Sergi Pascual-Guardia , Javier Gimeno , Dolores Naranjo , Laura Segalés , Silvia Hernández , Mercedes Simón , Laia Serrano , Beatriz Casado , Belén Lloveras & Joaquim Gea (21 Apr 2025): Muscle disease in severe COVID-19 patients: a microangiopathic myopathy, Ultrastructural Pathology, DOI: [10.1080/01913123.2025.2488809](https://doi.org/10.1080/01913123.2025.2488809)

**To link to this article:** <https://doi.org/10.1080/01913123.2025.2488809>



Published online: 21 Apr 2025.



Submit your article to this journal [↗](#)



View related articles [↗](#)



View Crossmark data [↗](#)



## Muscle disease in severe COVID-19 patients: a microangiopathic myopathy

Josep Lloreta-Trull<sup>a,b</sup>, Judith Marin-Corral<sup>c</sup>, Nuria Juanpere<sup>a,b</sup>, Sergi Pascual-Guardia<sup>b,d</sup>, Javier Gimeno<sup>a,b</sup>, Dolores Naranjo<sup>a</sup>, Laura Segalés<sup>a,b</sup>, Silvia Hernández<sup>a,b</sup>, Mercedes Simón<sup>a</sup>, Laia Serrano<sup>a</sup>, Beatriz Casado<sup>a</sup>, Belén Lloveras<sup>a,b</sup>, and Joaquim Gea<sup>b,d</sup>

<sup>a</sup>Department of Pathology, Hospital del Mar-Parc de Salut Mar, Institut Hospital del Mar d'Investigacions Mèdiques (IMIM), Barcelona, Spain;

<sup>b</sup>Department of Experimental and Health Sciences (CEXS), Universitat Pompeu Fabra, Barcelona, Spain; <sup>c</sup>Intensive Care Department, Hospital del Mar., Critical Pathology Research Group (GREPAC), IMIM, Barcelona, Spain; <sup>d</sup>Department of Respiratory Medicine, Hospital del Mar-IMIM, Barcelona, Spain

### ABSTRACT

Patients surviving coronavirus disease of 2019 (COVID-19) often complain of skeletal muscle weakness that may be very limiting and long-lasting. There are almost no studies on the skeletal muscle of these patients, and electron microscopic data are scarce. We assessed the ultrastructural changes in the quadriceps of eight patients with COVID-19 and found a combination of features different from those reported in corticosteroid myopathy and acute relaxant-steroid myopathy. The most remarkable and constant changes involved the endothelial cells and consisted of massive amounts of pinocytotic vesicles, degenerative changes, platelet aggregates and, most characteristic of all, an increase in the external lamina thickness that seems to stem from reduplication due to successive bouts of endothelial cell damage and subsequent regeneration. Viral particles were not found in any of the cases. This distinct and quite common set of alterations defines the myopathy associated with infection by severe acute respiratory syndrome coronavirus 2 (SARS-CoV-2). This association seems to be the result of an inflammatory process that would arise in infected cells but could damage non-infected endomysial blood vessels, thus resulting in persistent changes of the microvasculature that would be related to long-standing myopathic clinical features.

### ARTICLE HISTORY

Received 19 November 2024

Revised 7 March 2025

Accepted 1 April 2025

### KEYWORDS

COVID-19; early COVID-19; persistent COVID-19; skeletal muscle; myopathy; blood capillary; endomysium; external lamina thickening; external lamina reduplication

## Introduction

Widespread lung infiltration with features of Acute Respiratory Distress Syndrome is one of the most common and lethal forms of COVID-19.<sup>1–3</sup> Other less frequent but also potentially severe clinical presentations involve the gastrointestinal tract, heart, brain, liver, and kidney.<sup>3–6</sup> Muscle pain and weakness are present from the early stages and persist as a late manifestation of COVID-19 in a high percentage of patients, particularly in those with the most aggressive forms of the disease. Relatively little information is available on the origin, mechanisms, prevention, and treatment of this process.<sup>3,7</sup> Among the few papers dealing with this subject, some claim that muscle involvement would not be specifically related to SARS-CoV-2 infection, and that it would rather be a secondary event associated with intensive care treatment. Other authors suggest that this disorder is related to the primary involvement of nerve fibers, muscle cells, blood vessels, or loose connective

tissue, either as a result of the direct presence of the virus and/or of the subsequent inflammatory “storm.”<sup>8–10</sup> Dodig et al., in a study on three patients, report mainly changes in skeletal muscle cells. In their study, the authors claim to have found virus-like particles in necrotic muscle cells. While some of the images in this paper show quite convincing coronavirus particles, there are no clear features to support their location in muscle cells.<sup>8</sup> Two recent papers dealing with ultrastructural changes in the muscle biopsy of COVID-19 patients describe similar features in the external lamina of endomysial capillaries, but none of these papers contains a complete description on the series of changes involving mostly endothelial cells.<sup>8–10</sup>

We report on detailed ultrastructural findings in the quadriceps muscle from eight patients with severe COVID-19 and muscle-related symptoms. Although it is difficult to completely rule out some effect of the different drugs and Intensive Care

Unit (ICU) interventions on these patients, the spectrum of morphologic ultrastructural changes is quite unique and consistent, while the features that could be expected in a secondary myopathy are almost absent in most cases. We propose that muscle involvement in COVID-19 patients is a well-defined form of myopathy in which the main target of the injury is the endothelial cells of the endomy-sial blood vessels.

## Patients and methods

This study is based on the first eight consecutive patients with confirmed COVID-19 pneumonia admitted to our hospital and included in our main series. The patients were six men and two women, with a mean age of 65.8 years (range, 55–79 years). All of them had PCR-

proven COVID-19 with severe lung involve-ment, all but one required ICU admission, and three died of the disease (Table 1, Summary of clinical data).

The study was designed in accordance with our institution's ethical standards on human experi-mentation established in accordance with the 1964 helsinki Declaration and its subsequent amendments. Approval was granted by the Ethics Committee of Hospital del Mar-Parc de Salut Mar-Institut Hospital del Mar d'Investigacions Mèdiques (CEIC) (Ethics committee approval number: 2021/9783). Any details that might dis-close the subject's identity in the study were omitted. After informed consent from the patient or from a close relative with legal representation was obtained, an open biopsy was performed in the *vastus lateralis* of the quadriceps muscle.

**Table 1.** Summary of clinical data.

Table 1	Case #1	Case #2	Case #3	Case #4	Case #5	Case #6	Case #7	Case #8
<b>Days from symptoms to Biopsy</b>	7	10	13	21	21	22	29	45
<b>Demographics</b>								
Gender	M	M	M	M	F	M	F	M
Age, years	60	76	78	66	55	79	58	54
Body Mass Index, Kg/m <sup>2</sup>	32	24	28	27	23	29	29	29
<b>Comorbidities</b>								
Asthma	N	N	N	N	N	N	N	N
Chronic Obstructive Pulmonary Disease	N	Y	Y	N	N	N	N	N
Coronary disease	N	N	N	N	N	N	N	Y
Chronic Renal failure	N	N	Y	N	N	N	N	Y
Hypertension	Y	N	Y	Y	N	N	Y	Y
Diabetes Mellitus	Y	N	N	N	N	N	N	Y
Dyslipidemia	Y	N	N	Y	N	Y	N	N
Neoplasm	N	N	Y	N	N	N	N	N
Immunosuppression	N	N	N	N	N	N	N	Y
<b>Previous treatments</b>								
Statins	N	N	N	N	N	N	N	Y
Insulin	N	N	N	N	N	N	N	Y
Sistemic steroids	N	N	N	N	N	N	N	Y
<b>Respiratory support</b>								
Mechanical ventilation	Y	N	N	Y	Y	Y	Y	N
High flow nasal cannula	N	N	Y	Y	N	Y	N	Y
Non-invasive mechanical ventilation	Y	N	Y	N	Y	N	Y	Y
Tracheostomy	y	N	N	Y	Y			
<b>Analytical findings (day of biopsy was performed)</b>								
Leukocytes, u/mcl	5490	7130	12360	11340	10090	19810	15860	7990
Lynfocytes, u/mcl	430	650	370	900	750	420	1470	1560
C-Reactive Protein, mg/dl	6.40	0.96	12.69	8.29	1.12	7.52	0.72	5.15
D-Dimer, mcg/L	35200	3010	14890	2430	2850	7680	2300	—
<b>Treatments received previous to the biopsy</b>								
Neuromuscular blockers	Y	N	N	Y	Y	Y	Y	Y
Sedatives	Y	N	N	Y	Y	Y	Y	Y
Analgesia	Y	N	N	Y	Y	Y	Y	Y
Tocilizumab	N	N	N	N	Y	N	N	N
Systemic steroids	Y	Y	Y	Y	Y	Y	N	Y
Endovenous insulin	N	N	N	N	N	N	N	Y
Physical therapy	N	N	Y (Level 2)	Y (Level 1)	Y (Level 1)	Y (Level 2)	Y (Level 2)	Y (Level 2)
<b>Complications</b>								
Infection before the biopsy	N	N	Y	Y	Y	Y	Y	Y

Y: yes; N: no; Level 1: passive mobilization; Level 2: active-assisted exercises. Clinical features that could be related to muscle characteristics were also collected: days from symptoms to biopsy, demographics, comorbidities, previous treatments, respiratory support, analytical findings regarding inflammatory status when biopsy was performed, hospital treatments and infectious complications before biopsy was done.

Each sample was divided into three portions. One was fixed in formaldehyde for paraffin-based techniques: conventional Hematoxylin-Eosin, Masson's trichrome stains, and immunohistochemistry. Regarding the latter, specimens were stained with antibodies against collagen IV (prediluted mouse monoclonal primary antibody, clone CIV 22, VENTANA-Roche, Tucson, Arizona, USA), and against SARS-CoV-2 nucleoprotein (1:3000; polyclonal rabbit IgG, clone 40,143-T62, SinoBiological, Wayne, PA, USA), using the Optiview DAB IHC Detection kit and a BenchMark XT platform (VENTANA-Roche, Tucson, Arizona, USA). Fiber cross-sectional area (CSA) mean least diameter, and proportions of type I (expressing MHCI) and type II (expressing MHCII) fibers were also assessed by immunohistochemical analysis (clone MHC, Biogenesis Inc., Poole, UK, and clone MY-32, Sigma-Aldrich, Saint Louis, MO, USA) using a light microscope (Olympus, Series BX50F3, Olympus Optical Co., Hamburg, Germany) coupled with an image-digitizing camera (Pixera Studio, version 1.0.4; Pixera Corporation, Los Gatos, CA), and subsequently evaluated using a specific morphometry program (Image J, U. S. National Institutes of Health, Bethesda, Maryland, USA). At least 150 fibers were measured and counted in each muscle specimen.

A second portion was mounted on a flat cork support and snap-frozen in isopentane cooled by immersion in liquid nitrogen and stored at  $-80^{\circ}\text{C}$  in the tissue bank. Finally, the samples for electron microscopy that are the base of the present study were first immersed in 2% neutral buffered glutaraldehyde "in toto" to allow the tissue to immediately start fixation and increase tissue resistance to compression. After that, the tissue was minced in cubes of less than 1 mm in their largest dimension using a fresh scalpel. These fragments were then fixed overnight in glutaraldehyde and postfixed in osmium tetroxide for 1 hour. After eliminating osmium residues with three cacodylate buffer rinses and dehydrating the samples with a series of ethanol (70, 95, 100, 100%), and two pure acetone changes, the tissue was embedded in epoxy resin. The resulting blocks were cut, and 1  $\mu\text{m}$  sections from each block were stained with toluidine blue. The blocks with the best orientation and the more apparent light microscopic changes were selected for thin-sectioning with a diamond knife,

mounted in copper grids, and stained with uranyl acetate and lead citrate. These sections were examined in a FEI (Thermo-Fisher) CM100 transmission electron microscope at an accelerating voltage of 80kv. A systematic screening was performed in all sections from the different blocks, and the coordinates of all the areas of interest were stored and subsequently analyzed. Information on all the muscle biopsy compartments was recorded following a preset protocol. A descriptive summary table was prepared with all the data. The intensity and extension of the ultrastructural findings were graded in a four tier scale: 0 = not present; 1 = mild, 2 = moderate, and 3 = severe. Electron micrographs were taken from the most representative findings.

## Results

By light microscopy, there were only occasional atrophic muscle fibers, without necrotic foci nor inflammatory cell infiltrates. The overall proportion of type I and type II muscle fibers was 45%:55%, and there were no apparent differences in muscle fiber diameter. Isolated foci of mild endomysial widening were also found.

Upon ultrastructural examination, the most striking features in all cases involved the endomysial blood vessels, and they could be arranged in a probable sequence of events. The earliest change was a marked increase in pinocytotic vesicles on both the luminal and the stromal aspect of the endothelial cells (Figure 1(a)). Intracellular edema and degenerative changes were identified in three of the cases (Figure 1(b)), without any associated inflammatory infiltrate. Platelet aggregates, with and without micro-thrombi formation, were found in three cases. Finally, the most constant and distinctive finding was the reduplication of the external lamina of endothelial cells. In the earlier images, there was marked separation of the different layers, with interposed amorphous stromal matrix and sometimes cell debris (Figure 2(a)). Later, these layers were densely packed and eventually the multilayering almost disappeared, resulting in a homogeneously dense and markedly thickened external lamina (Figures 2(b) and 3). Different stages coexisted in the same cases, ranging from slightly thickened to massive external lamina (Figure 4). These ultrastructural findings



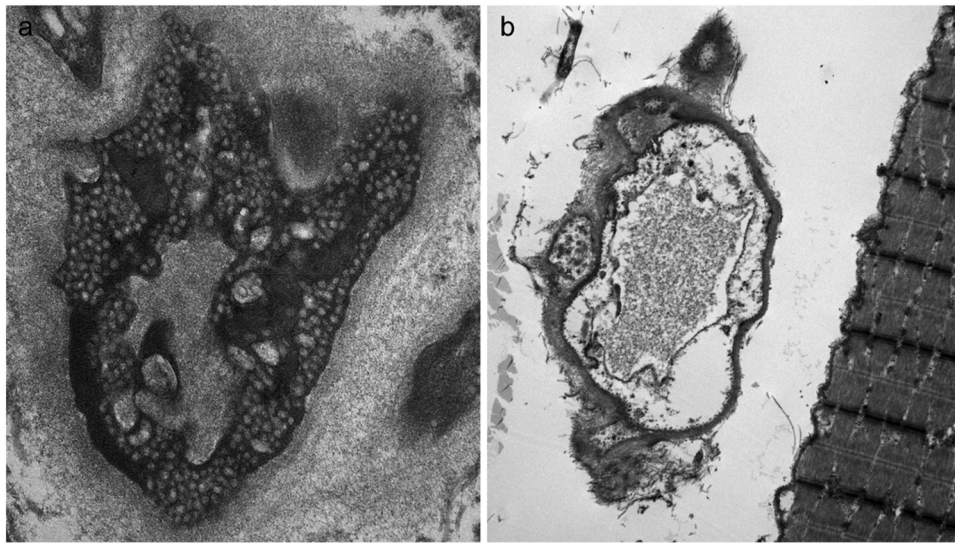


**Figure 1.** Ultrastructural changes in endothelial cells of the endomysial capillaries. (a), very abundant pinocytotic vesicles fill not only the luminal and basal aspects of the endothelial cells but also apparently occupy part of their cytoplasm. Original magnification  $\times 34,000$ . (b), endomysial capillary showing prominent swelling of the endothelial cells, with preservation of the luminal cell membrane and marked clearing of all the cytoplasmic contents due to massive intracellular edema. A normal appearing skeletal muscle fiber can be seen in the right side of this micrograph. Original magnification  $\times 7,900$ .

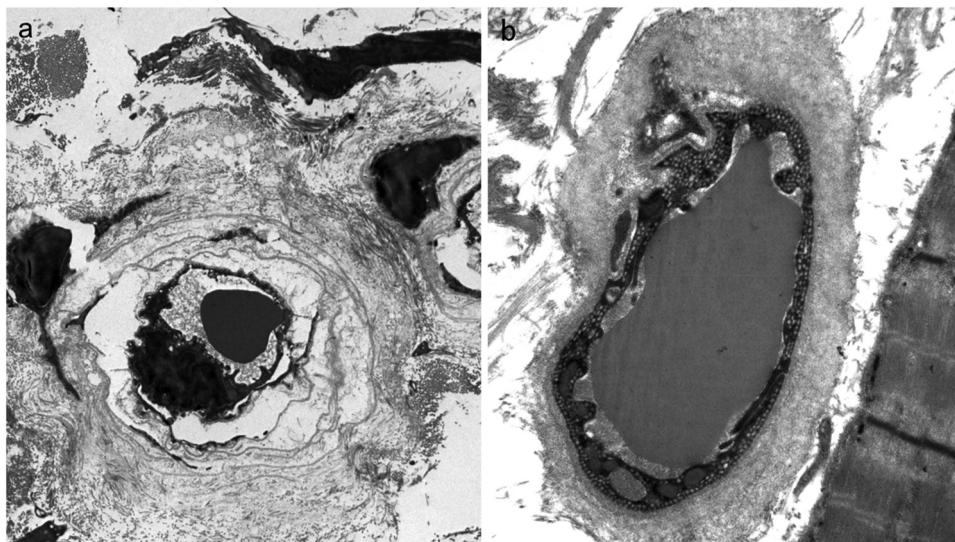


**Figure 2.** Electron microscopic images of early and late multilayering in the external lamina of the endomysial capillaries. (a), initial lesions consisted of loose concentric lamellae of endothelial external lamina, with interspersed amorphous extracellular matrix among the leaflets. Original magnification  $\times 5,800$ . (b), in later stages, a progressive compaction of the leaflets with reduction of the amount of extracellular matrix among them was observed, resulting in a more homogeneous and usually prominent thickening of the external lamina. Again, an apparently normal skeletal muscle fiber is present in the right side of the image. Original magnification  $\times 10,500$ .

could also be appreciated by light microscopy with anti-collagen IV immunostaining (Figure 5).

Regarding the abnormalities in skeletal muscle fibers, they consisted mainly in edema and non-specific degenerative and reactive changes and were focal and milder in comparison to blood

vessel involvement (Figure 6). For additional information on ultrastructural changes, see Table 2 (Summary of ultrastructural findings). SARS-CoV-2 viral particles were not found either by transmission electron microscopy or by immunohistochemistry (Figure 7).

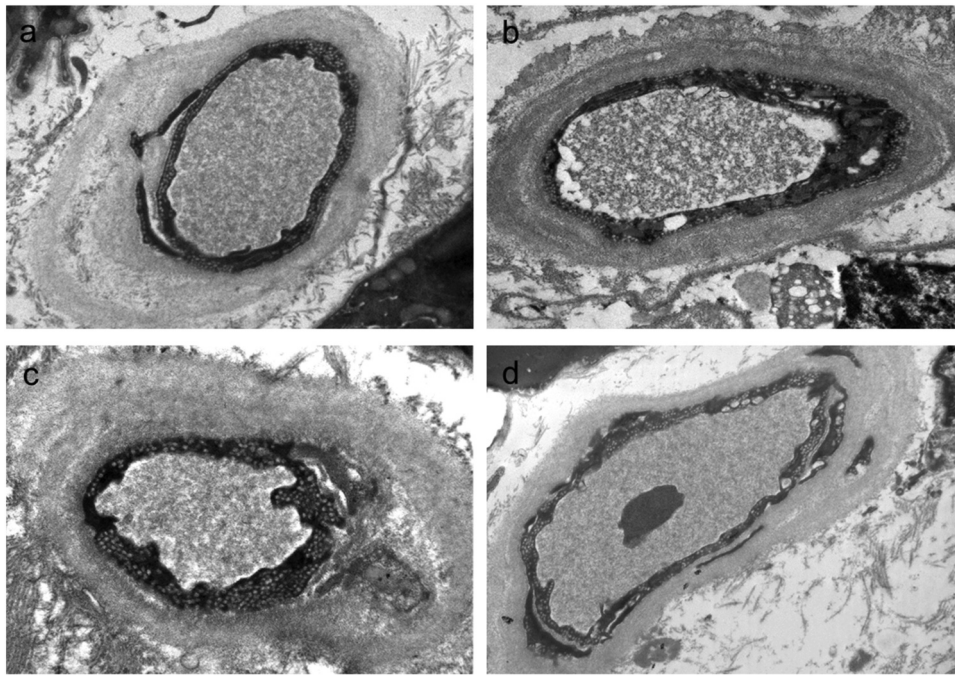


**Figure 3.** Images of increasing compaction of the leaflets of external lamina could be traced from the earliest loose leaflet deposition (main text [Figure 2\(a\)](#)) to more diffuse and homogeneous external lamina thickening. The amount of more electron lucent matrix among the leaflets was progressively reduced. Original magnifications: (a), (b) and (d): x10,500; (c) x19,000.

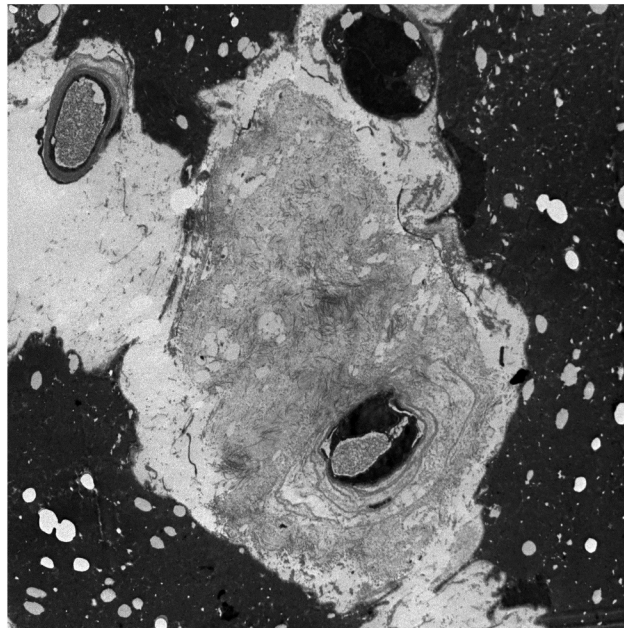


**Figure 4.** Electron micrograph illustrating the overlap of different processes in the same specific time-point. Thus, it is possible to appreciate how some capillaries had still minimal thickening of the external lamina (upper left corner), while others had a markedly increased amount of external lamina material around them showing simultaneous degenerative changes in the endothelial cells (center of the image). Original magnification x3,400.



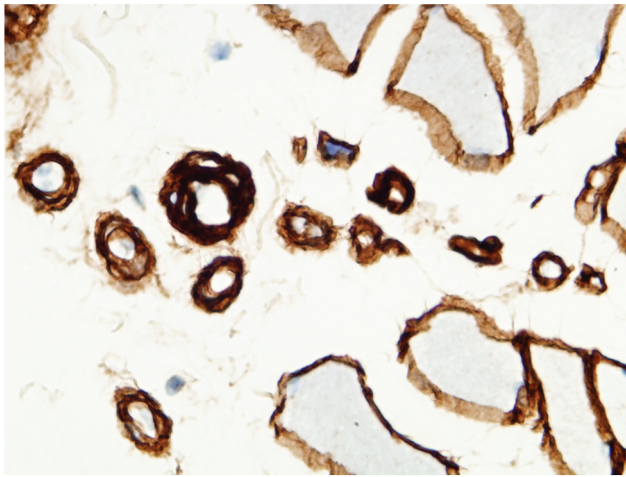


**Figure 5.** Immunohistochemical stain for collagen IV showing variable degrees of lamina externa thickening and multilamellation in endomyisial capillaries (x500).

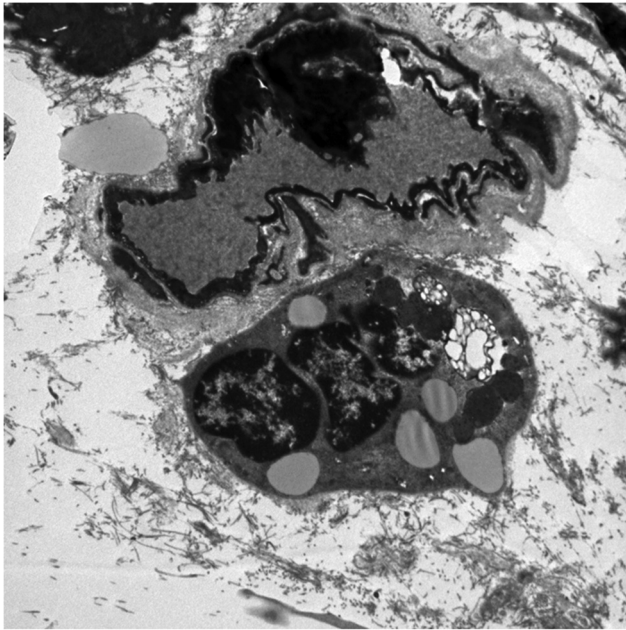


**Figure 6.** Electron micrograph showing an extremely atrophic muscle fiber (center of the image) with almost no contractile elements and with clustered nuclei, adjacent to a dilated capillary (above). Original magnification  $\times 7,900$ .

## Discussion

Muscle weakness can be observed in the first days of the disease, but it is mostly a late manifestation of COVID-19. It targets a high percentage of patients surviving COVID-19, particularly those with the most severe forms of this disease. However, relatively little information is available on the origin and mechanisms of this process.<sup>3,7</sup>

There are several etiopathogenic hypotheses, but they still have limited supporting evidence. Moreover, while the number of articles on COVID-19 is progressively increasing, those on its associated muscle involvement are scarce and do not include a complete morphological description of the changes in the different muscle tissue components.<sup>8–10</sup> To the best of our knowledge, this is one of the first systematic and detailed reports of the ultrastructural changes present in the muscle of patients with severe COVID-19. The results of this study favor the possibility of microangiopathy as the main origin of muscle involvement. However, several possible factors can contribute to the skeletal muscle damage in COVID-19 patients, particularly in the severe forms of the disease requiring intensive care unit admission.

One of the most obvious alternative mechanisms of muscle involvement in COVID-19 is deconditioning derived from the reduction in physical activity.<sup>11–15</sup> However, although this could be a contributing factor in our patients, the predominant changes in deconditioned muscles consist of marked and generalized fiber atrophy, associated with signs of damage and even autophagy, while their regenerative capacity decreases.<sup>16,17</sup> These findings differ from the main features in the present series. Moreover, if deconditioning was an important factor, the duration of the admission would be proportional to the intensity of the damage. Nevertheless, in our series, the damage appears early on and persists throughout the course of the disease with similar intensity once the complete pathogenic sequence has been established, i.e. when the external lamina compaction stage has been reached.

As in other organs, the SARS-CoV-2 virus could directly damage skeletal muscle. In this regard, we have not detected viral particles, either after very extensive ultrastructural screening or by immunohistochemistry. The damage could also be the result of a systemic inflammatory response induced by the virus. This mechanism is considered to be responsible for many of the most deleterious effects of COVID-19 disease.<sup>3</sup> The fact that the endothelial cell is the main target of the skeletal muscle involvement, the lack of inflammatory infiltrate and the presence of increased amounts of platelets and of small thrombi, all would be in keeping with the

**Table 2.** Summary of ultrastructural findings.

	Case #1	Case #2	Case #3	Case #4	Case #5	Case #6	Case #7	Case #8
<b>Viral particles</b>	0	0	0	0	0	0	0	0
<b>Endomysial capillaries</b>								
Endothelial swelling	3	2	0	0	0	0	2	0
Endothelial degeneration-necrosis	0	2	0	0	0	1	2	0
Endothelial massive pynocytosis	3	3	1	3	2	3	1	2
Intracapillary platelet clusters	2	0	0	0	0	1	3	0
Microthrombi	0	0	1	0	0	1	3	0
Capillary. fragmentation	0	0	0	0	0	0	1	0
Reduplication of external lamina	2	2	1	2	1	2	1	3
Compaction external lamina	3	3	2	3	2	3	1	3
Thickening of external lamina	3	3	3	3	2	3	2	3
Electrondense deposit-like acumulations	1	0	0	0	0	0	0	0
<b>Skeletal Muscle cell</b>								
Edema	1	1	0	0	1	1	1	1
Atrophy	1	1	1	2	1	2	0	2
Increased lipofuscin	3	2	1	2	1	1	0	1
Sarcolemmal disorganization	1	1	1	1	1	1	1	1
Degeneration	1	1	0	0	1	1	0	0
Sarcomeric spheroids	0	0	0	1	0	0	0	0
Reticulum swelling	0	0	0	0	0	0	0	0
Sarcoplasm swelling	0	0	0	1	0	0	1	1
Lipid increase	0	0	2	1	0	0	0	2
<b>Total</b>	24	21	12	19	12	20	19	19

0: not present; 1: mild; 2: moderate; 3: severe.

possibility of systemic or local microangiopathy, damaging capillaries without the direct local involvement of the virus.

In addition to the already mentioned changes in blood vessels, there was a spectrum of nonspecific findings in adjacent skeletal muscle fibers. *Overall fiber structure*: while some of the muscle fibers were strictly normal in size and shape, there were several fibers with atrophy of different intensity in all cases. The most atrophic of them were reduced to very small cells with scant cytoplasm, almost without sarcomeres, and with nuclear clusters. In other cases, the normal structure was preserved, but the fibers had a small diameter, ruffled sarcolemma, and increased density of the cytoplasm. *Nuclei*: muscle cell nuclei were usually of normal size and distribution, but many of them showed rather prominent nucleolus. Moreover, there were occasional clusters of 2–3 nuclei. However, nuclear internalization was rarely observed. *sarcomeres*: most of them were normal in size and structure. In two cases, there was one isolated spheroidal inclusion similar to those that can be observed in inclusion body myositis, but with some features that suggested that they were misshaped sarcomeres in which the rounded contour resulted in an abnormal outline of the cell surface. *Mitochondria*: although there were isolated mitochondrial clusters, this was not

a remarkable finding in most of the cases. *T tubules, sarcoplasmic reticulum, and sarcoplasm*: some muscle fibers had sarcoplasmic swelling due to edema, but there was no significant dilation nor any other remarkable morphologic abnormality of the sarcoplasmic reticulum or the T tubular system. *Lipids*: there were no remarkable differences in lipid content or droplet size among the oxidative or the glycolytic fibers. *Glycogen*: there were some glycogen pools, but they were small and occasional. *Inclusions and abnormal structures*: in some of the affected fibers either with cytoplasmic swelling or atrophy, there was an increase in the clusters of lipofuscin aggregates. *External lamina and sarcolemmal membrane*: only one fiber of one case had focal reduplication of the external lamina. Interestingly, some muscle fibers were seen to project pseudopod-like processes that apparently were aimed at interstitial blood vessels. This feature was observed in two cases. *Nerve fibers and motor plates*: in spite of having sectioned all the blocks, no nerve fibers or motor endplates were found.

Corticosteroid myopathy, as well as acute relaxant-steroid myopathy (ARSM) found in intensive care unit patients undergoing mechanical ventilation, could also be superimposed in these patients. Nevertheless, the ultrastructural morphologic spectrum in these disorders, mostly



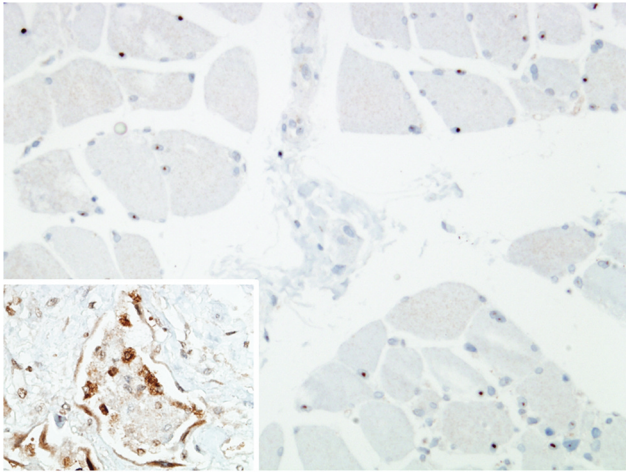


**Figure 7.** Negative anti-SARS-CoV-2 nucleoprotein stain in skeletal muscle. some nuclei showed an aberrant dot-like staining ( $\times 200$ ). Inset: positive control consisting of a lung alveolus with cytoplasmic staining in pneumocytes. Degenerating cells in the alveolar lumen are probably the result of shedding of the alveolar cell lining ( $\times 400$ ). No viral particles were identified in any of the patients by transmission electron microscopy after extensive sampling of the muscle tissue. A detailed screening was performed in the whole surface of all the available sections, including all cell types present in them (endothelial cells, pericytes, muscle cells, satellite cells, fibroblasts, macrophages and other inflammatory cells). For this analysis, previous positive samples obtained in our lab from other tissues were used as reference images. In addition, we considered a checklist of possible pitfalls, including tangential sections of rough endoplasmic reticulum, irregular or mottled pinocytotic vesicles, clathrin-covered vesicles, golgi-derived vesicles, artifactual membranous incomplete structures, and multivesicular bodies. There were no structures with the minimal morphologic criteria to be considered consistent with the presence of coronavirus in any of the samples included in the study.

muscle fiber necrosis with some degree of capillary degeneration, mitochondrial crystalline inclusions and also the cytoplasmic nemaline rods observed in ARSM, is quite different from the range of alterations seen in our patients.<sup>11–13,15</sup> With regard to hydroxychloroquine-related myopathy, again the ultrastructural changes would have been quite different and, furthermore, none of our eight patients had been treated with this drug.<sup>14</sup>

Although it is not possible to absolutely rule out the possibility that some of the aforementioned factors can be contributory in patients with COVID-19 myopathy, we conclude that the findings in our series are robust and constant enough to define a peculiar form of chronic SARS-CoV-2-related myopathy.

The most striking and constant ultrastructural features observed in the present study involve endothelial cells and their external lamina. In a logical sequence, the first change would have been the massive pinocytotic vesicle formation within the endothelial cells. This feature is generally observed in tissues with enhanced metabolic activity. The increased activity of the endothelial cells could be linked to the presence of viral particles, but we have not been able to find any reliable images to support this hypothesis.<sup>18</sup> Nevertheless, it seems that this altered metabolism could result in an energetic overload,<sup>16</sup> with or without a combined immunological response, which would eventually damage the endothelial cells. At this point, they would become swollen, and their viability would be compromised, resulting in the images of intracellular edema and cytolysis seen in our patients. Moreover, after every bout of endothelial cell injury, regeneration would ensue, giving rise to the early changes in the external lamina consisting in varying degrees of multilamination. This change is reminiscent of the external lamina reduplication seen in peritubular capillaries of the kidney in cases of chronic antibody-mediated organ rejection.<sup>19,20</sup> This feature has also been reported in other situations, such as the synovium of rheumatoid arthritis, or the microcirculation of many organs in diabetic patients.<sup>21,22</sup> Furthermore, in the specific case of kidney transplantation, this finding is associated with an immunological response that damages the endothelial cells through serum complement activation. In rheumatoid arthritis, the basis of endothelial cell damage is also related to immunological or inflammatory mechanisms. In diabetes, the underlying mechanism is not well understood, but it is obvious that the target in this disease is also the endothelial cell. In all these cases, the external lamina persists despite the injury to the endothelial cell. Thus, every new set of regenerated endothelial cells would produce a new layer of external lamina, and therefore the number of layers could be considered a reflection of the number of damage cycles. Importantly, in all these disorders the endothelial cell is destroyed by cytolysis rather than by necrosis, and this type of cell death is not usually associated with an inflammatory response. In this regard, it is worth emphasizing that the

absence of inflammatory cells is also a feature of our cases. Otherwise, in the event of a conventional inflammatory infiltrate, the stromal components would be more intensely remodeled and instead of a reduplicated external lamina, the healing process would have resulted in fibrous scarring of the tissue.

Regarding the microangiopathy of diabetes mellitus, multilayering of the external lamina has been reported in the capillaries of skeletal muscle.<sup>22</sup> In the published images, the lamellation is always of the compact type rather than loose and asymmetric, as it is in our cases. According to our experience from muscle and from kidney, this is not a usual finding, as most cases of diabetic nephropathy and neuropathy, as well as most muscle samples of advanced diabetic patients, show a marked but homogeneous thickening of the external lamina.<sup>22</sup>

In the present series of skeletal muscle samples from COVID-19 patients, the early images would be reminiscent of an immunologically mediated process, while in later stages the findings would be like those of a metabolic disorder similar to diabetes. The consequences of the marked thickening of the external lamina in COVID-19 patients are not fully understood, but it could be speculated that impaired oxygen diffusion to the endomysial loose connective tissue would ensue.<sup>23</sup> This would result in local hypoxia that would target the most oxygen-dependent structures in the muscle tissue, namely nerve fibers, motor plates, and oxidative (type I) skeletal muscle fibers.

In conclusion, according to the results of the present study, damage of the endothelial cells of the endomysial capillaries is the main event in the limiting and usually long-lasting muscle involvement of COVID-19 patients. Although it is difficult to completely exclude the potential role of intensive care-related toxicities and co-morbidities, we propose that this set of events defines a new form of myopathy, characteristic of SARS-CoV-2 infection, the COVID-19 myopathy.

### Author contributions

CRedit: **Josep Lloreta-Trull**: Conceptualization, Data curation, Formal analysis, Investigation, Methodology, Project administration, Resources, Software, Supervision, Validation,

Visualization, Writing – original draft, Writing – review & editing; **Judith Marin-Corral**: Data curation, Investigation, Methodology; **Nuria Juanpere**: Conceptualization, Data curation, Investigation, Writing – review & editing; **Sergi Pascual-Guardia**: Data curation, Formal analysis, Investigation, Methodology, Writing – review & editing; **Javier Gimeno**: Conceptualization, Investigation, Supervision, Writing – review & editing; **Dolores Naranjo**: Investigation, Methodology, Writing – review & editing; **Laura Segalés**: Data curation, Investigation, Methodology, Writing – original draft; **Silvia Hernández**: Conceptualization, Investigation, Methodology, Writing – review & editing; **Mercedes Simón**: Investigation, Methodology, Resources, Writing – review & editing; **Laia Serrano**: Data curation, Investigation, Resources, Writing – review & editing; **Beatriz Casado**: Investigation, Methodology, Resources, Writing – review & editing; **Belén Lloveras**: Conceptualization, Methodology, Resources, Writing – review & editing; **Joaquim Gea**: Conceptualization, Data curation, Resources, Supervision, Validation, Writing – review & editing.

### Disclosure statement

No potential conflict of interest was reported by the author(s).

### Funding

The author(s) reported there is no funding associated with the work featured in this article.

### References

1. Bradley BT, Maioli H, Johnston R, et al. Histopathology and ultrastructural findings of fatal COVID-19 infections in Washington State: a case series. *Lancet*. 2020;396(10247):320–332. doi: [10.1016/S0140-6736\(20\)31305-2](https://doi.org/10.1016/S0140-6736(20)31305-2).
2. Hariri L, Hardin CC. Covid-19, Angiogenesis, and ARDS Endotypes. *N Engl J Med*. 2020;383(2):182–183. doi: [10.1056/NEJMe2018629](https://doi.org/10.1056/NEJMe2018629).
3. Polak SB, Van Gool IC, Cohen D, Von Der Thüsen JH, Van Paassen J. A systematic review of pathological findings in COVID-19: a pathophysiological timeline and possible mechanisms of disease progression. *Mod Pathol*. 2020;33(11):2128–2138. doi: [10.1038/s41379-020-0603-3](https://doi.org/10.1038/s41379-020-0603-3).
4. Puelles VG, Lütgehetmann M, Lindenmeyer MT, et al. Multiorgan and renal tropism of SARS-CoV-2. *N Engl J Med*. 2020;383(6):590–592. doi: [10.1056/NEJMc2011400](https://doi.org/10.1056/NEJMc2011400).
5. Su H, Yang M, Wan C, et al. Renal histopathological analysis of 26 postmortem findings of patients with COVID-19 in China. *Kidney Int*. 2020;98(1):219–227. doi: [10.1016/j.kint.2020.04.003](https://doi.org/10.1016/j.kint.2020.04.003).

6. Wang W, Xu Y, Gao R, et al. Detection of SARS-CoV-2 in different types of clinical specimens. *JAMA*. 2020;323:1843–1844. doi: [10.1001/jama.2020.3786](https://doi.org/10.1001/jama.2020.3786).
7. Letko M, Marzi A, Munster V. Functional assessment of cell entry and receptor usage for SARS-CoV-2 and other lineage B betacoronaviruses. *Nat Microbiol*. 2020;5(4):562–569. doi: [10.1038/s41564-020-0688-y](https://doi.org/10.1038/s41564-020-0688-y).
8. Dodig D, Tarnopolsky MA, Margeta M, Gordon K, Fritzler MJ, Lu JQ. COVID-19-associated critical illness myopathy with direct viral effects. *Ann Neurol*. 2022;91(4):568–574. doi: [10.1002/ana.26318](https://doi.org/10.1002/ana.26318).
9. Aschman T, Schneider J, Greuel S, et al. Association between SARS-CoV-2 infection and immune-mediated myopathy in patients who have died. *JAMA Neurol*. 2021;78:948–960. doi: [10.1001/jamaneurol.2021.2004](https://doi.org/10.1001/jamaneurol.2021.2004).
10. Hejbøl EK, Harbo T, Agergaard J, et al. Myopathy as a cause of fatigue in long-term post-COVID-19 symptoms: evidence of skeletal muscle histopathology. *Eur J Neurol*. 2022;29(9):2832–2841. doi: [10.1111/ene.15435](https://doi.org/10.1111/ene.15435).
11. Eddelien HS, Hoffmeyer HW, Lund EL, Lauritsen AØ. Glucocorticoid-induced myopathy in the intensive care unit. *BMJ Case Rep*. 2015;2015:1–3. doi: [10.1136/bcr-2015-209793](https://doi.org/10.1136/bcr-2015-209793).
12. Hanson P, Dive A, Brucher JM. Acute corticosteroid myopathy in intensive care patients. *Muscle Nerve*. 1997;20:1371–1380. doi: [10.1002/\(sici\)1097-4598\(199711\)20:11<1371:aid-mus4>3.0.co;2-7](https://doi.org/10.1002/(sici)1097-4598(199711)20:11<1371:aid-mus4>3.0.co;2-7).
13. Ramsay DA, Zochodne DW, Robertson DM, Nag S, Ludwin SK. A syndrome of acute severe muscle necrosis in intensive care unit patients. *J Neuropathol Exp Neurol*. 1993;52(4):387–398. doi: [10.1097/00005072-199307000-00006](https://doi.org/10.1097/00005072-199307000-00006).
14. Costa RM, Martul EV, Reboredo JM, Cigarrán S. Curvilinear bodies in hydroxychloroquine-induced renal phospholipidosis resembling Fabry disease. *Clin Kidney J*. 2013;6(5):533–536. doi: [10.1093/ckj/sft089](https://doi.org/10.1093/ckj/sft089).
15. Matsubara S, Kitaguchi T, Isozaki E, Miyamoto K, Hirai S. Changes in the cytoskeletal proteins, sarcoplasmic reticulum, and capillaries in acute relaxant-steroid myopathy (ARSM) in contrast to the corticosteroid myopathy. *Acta Neuropathol*. 1999;97(5):515–519. doi: [10.1007/s004010051022](https://doi.org/10.1007/s004010051022).
16. Gea J, Pascual S, Casadevall C, Orozco-Levi M, Barreiro E. Muscle dysfunction in chronic obstructive pulmonary disease: update on causes and biological findings. *J Thorac Dis*. 2015;7:418–438. doi: [10.3978/j.issn.2072-1439.2015.08.04](https://doi.org/10.3978/j.issn.2072-1439.2015.08.04).
17. Puig-Vilanova E, Rodriguez DA, Lloreta J, et al. Oxidative stress, redox signaling pathways, and autophagy in cachectic muscles of male patients with advanced COPD and lung cancer. *Free Radic Biol Med*. 2015;79:91–108. doi: [10.1016/j.freeradbiomed.2014.11.006](https://doi.org/10.1016/j.freeradbiomed.2014.11.006).
18. Goldsmith CS, Miller SE, Martines RB, Bullock HA, Zaki SR. Electron microscopy of SARS-CoV-2: a challenging task. *Lancet*. 2020;395(10238):e99. doi: [10.1016/S0140-6736\(20\)31188-0](https://doi.org/10.1016/S0140-6736(20)31188-0).
19. Drachenberg CB, Steinberger E, Hoehn-Saric E, et al. Specificity of intertubular capillary changes: comparative ultrastructural studies in renal allografts and native kidneys. *Ultrastruct Pathol*. 1997;21(3):227–233. doi: [10.3109/01913129709021918](https://doi.org/10.3109/01913129709021918).
20. Lajoie G. Antibody-mediated rejection of human renal allografts: an electron microscopic study of peritubular capillaries. *Ultrastruct Pathol*. 1997;21(3):235–242. doi: [10.3109/01913129709021919](https://doi.org/10.3109/01913129709021919).
21. Matsubara T, Ziff M, Smith A. Basement membrane thickening of postcapillary venules and capillaries in rheumatoid synovium. Immunoelectron microscopic and electron microscopic morphometric analysis. *Arthritis Rheum*. 1987;30(1):18–30. doi: [10.1002/art.1780300103](https://doi.org/10.1002/art.1780300103).
22. Vracko R, Beneditt EP. Manifestations of diabetes mellitus--their possible relationships to an underlying cell defect. A review. *Am J Pathol*. 1974;75(1):204–224.
23. Maina JN, West JB. Thin and strong! The bioengineering dilemma in the structural and functional design of the blood-gas barrier. *Physiol Rev*. 2005;85(3):811–844. doi: [10.1152/physrev.00022.2004](https://doi.org/10.1152/physrev.00022.2004).